A PRELIMINARY THERMAL DISTORTION ANALYSIS

OF THE

PROPOSED AOSO EXPERIMENT SUPPORT STRUCTURE

By Donald E. Gray

Goddard Space Flight Center
Greenbelt, Maryland

Summary 14913

A mathematical model of one experiment ideally mounted to the experiment support tube is considered. A set of compatibility equations is developed and expanded to determine expressions for interaction loads and rotational deflections. Two digital computer programs are developed to undertake a host of thermal inputs for various experiment sizes and mounting locations.   *Author*

iii

CONTENTS

Symbols

$\{\delta_T\}$ temperature induced displacement and rotation matrix for the experiment

$\{\bar{\delta}_T\}$ temperature induced displacement and rotation matrix for the hexagonal support tube

$[f]$ influence coefficient matrix for loads applied at the neutral axis of the experiment

$[\bar{f}]$ influence coefficient matrix for loads applied at the neutral axis of the hexagonal support tube

$\{X\}$ matrix of loads acting off the experiment neutral axis and referenced to the neutral axis of the experiment

$\{\bar{X}\}$ matrix of loads acting off the hexagonal support tube neutral axis and referenced to the neutral axis of the hexagonal support tube

$\delta_{\phi\bar{P}}$ rotational deflection of point $\bar{P}$ with respect to point $\bar{P}'$, radians (Figure 3)

$\delta_{\phi\bar{P}''}$ rotational deflection of point $\bar{P}''$ with respect to point $\bar{P}'$, radians (Figure 3)

$\delta_{\phi\bar{P}''/\bar{P}}$ rotational deflection of point $\bar{P}''$ with respect to point $\bar{P}$, radians (Figure 3)

L distance between forward experiment mount and assumed cantilevered point, in

L' length of hexagonal support tube subjected to free bending, in

The following symbols, where capped with a bar (-), refer to the hexagonal support tube.

α coefficient of linear thermal expansion of experiment housing, in/in/°F

E modulus of elasticity of experiment housing, psi

I cross sectional moment of inertia of experiment housing, in^4

T uniform temperature of experiment referenced to a datum temperature, °F

ΔT transverse linear thermal gradient applied across experiment, °F

A cross sectional area of experiment housing, in^2

h depth of experiment housing, in

X_H horizontal reaction induced at forward experiment mount, lb

X_V vertical reaction induced at forward experiment mount, lb

X_M moment induced at forward experiment mount, in-lb

A PRELIMINARY THERMAL DISTORTION ANALYSIS

OF THE

PROPOSED AOSO EXPERIMENT SUPPORT STRUCTURE

by
Donald E. Gray

INTRODUCTION

One of the primary objectives of the Advanced Orbiting Solar Observatory (AOSO) structural subsystem is to satisfy and maintain the stringent optical alignment requirements established between sun sensors and certain of the contemplated experiments. The spacecraft substructure pertinent to this objective is the central experiment support tube.

The proposed experiment support tube is an aluminum alloy hexagonal cylinder composed of six joined honeycomb sandwich panels. The hexagonal tube is joined to the external observatory structure through three radial pylon supports which are attached to the tube at its midspan. Proposed experiment mounting to the support tube is through two yoke end mounts which are joined by four diagonal struts.

The optical misalignment induced between sun sensors and individual experiments is a function of both geometric and thermal variables. For an assumed geometric configuration and zero "g" environment, the optical misalignments can be attributed primarily to the temperature gradients over, and temperature levels of, both the support tube and the experiments.

DISCUSSION

It is of first interest to obtain some estimate of the interaction loads induced at the experiment mounts by experiment interaction with the support tube. As shown in Figure 1, a single experiment is considered mounted to the top of the support tube and left of its midspan. The thermal gradients applied across the experiment and tube are assumed linear and constant over the length of the structure between mount locations. The Euler-Bernoulli theory is assumed and the experiment and tube are considered cantilevered at the aft (right) mount. It is further assumed that no relative rotations or displacements occur at the mounts.

Considering the deflections of points P and $\bar{P}$ (see Figure 1) and applying the above assumptions, a set of compatibility equations can be developed in terms of interaction loads at the forward

experiment mount. The sign convention used for deflections, loads, and temperature gradients is depicted in Figure 2. Also shown are the loads at points P and $\bar{P}$. In matrix form, the compatibility equation is

$$\{\delta_T\} + [f]\{X\} = \{\bar{\delta}_T\} + [\bar{f}]\{\bar{X}\} \tag{1}$$

Since $\bar{X}_H = -X_H$, $\bar{X}_V = -X_V$, and $\bar{X}_M = -X_M$, Equation (1) can be expanded to

$$
\begin{Bmatrix}
\alpha L\left(T + (\Delta T)/2\right) \\[2mm]
\alpha L^2 \Delta T/2h \\[2mm]
-\alpha L\Delta T/h
\end{Bmatrix}
+
\begin{bmatrix}
L/AE & L^2 h/4EI & -Lh/2EI \\[2mm]
0 & L^3/3EI & -L^2/2EI \\[2mm]
0 & -L^2/2EI & L/EI
\end{bmatrix}
\begin{Bmatrix}
X_H \\[2mm]
X_V \\[2mm]
X_M - \left(X_H h\right)/2
\end{Bmatrix}
$$

$$
=
\begin{Bmatrix}
\bar{\alpha}L\left(\bar{T} - (\Delta\bar{T})/2\right) \\[2mm]
\bar{\alpha}L^2 \overline{\Delta T}/2\bar{h} \\[2mm]
-\bar{\alpha}L\overline{\Delta T}/\bar{h}
\end{Bmatrix}
-
\begin{bmatrix}
L/\overline{AE} & -L^2 \bar{h}/4\overline{EI} & L\bar{h}/2\overline{EI} \\[2mm]
0 & L^3/3\overline{EI} & -L^2/2\overline{EI} \\[2mm]
0 & -L^2/2\overline{EI} & L/\overline{EI}
\end{bmatrix}
\begin{Bmatrix}
X_H \\[2mm]
X_V \\[2mm]
X_M + \left(X_H \bar{h}\right)/2
\end{Bmatrix}
\tag{2}
$$

The individual terms of Equation (2) are developed in Appendix A.

The influence coefficient matrices are unsymmetrical due to the non-zero terms f_{12} and f_{13}. Both terms must be considered since points P and $\bar{P}$ are at substantial distances from their respective neutral axis.

Adjusting the influence coefficient matrices in Equation (2), the load column matrix can be rewritten in terms of the three primary reaction loads X_H, X_V, and X_M. Thus

$$
\begin{Bmatrix}
\alpha L\left(T + (\Delta T)/2\right) \\[2mm]
\alpha L^2 \Delta T/2h \\[2mm]
-\alpha L\Delta T/h
\end{Bmatrix}
+
\begin{bmatrix}
\left(L/AE + Lh^2/4EI\right) & L^2 h/4EI & -Lh/2EI \\[2mm]
L^2 h/4EI & L^3/3EI & -L^2/2EI \\[2mm]
-Lh/2EI & -L^2/2EI & L/EI
\end{bmatrix}
\begin{Bmatrix}
X_H \\[2mm]
X_V \\[2mm]
X_M
\end{Bmatrix}
$$

$$
=
\begin{Bmatrix}
\bar{\alpha}L\left(\bar{T} - (\Delta\bar{T})/2\right) \\[2mm]
\bar{\alpha}L^2\overline{\Delta T}/2\bar{h} \\[2mm]
-\bar{\alpha}L\overline{\Delta T}/\bar{h}
\end{Bmatrix}
-
\begin{bmatrix}
\left(L/\overline{AE} + L\bar{h}^2/4\overline{EI}\right) & -L^2 \bar{h}/4\overline{EI} & L\bar{h}/2\overline{EI} \\[2mm]
-L^2 \bar{h}/4\overline{EI} & L^3/3\overline{EI} & -L^2/2\overline{EI} \\[2mm]
L\bar{h}/2\overline{EI} & -L^2/2\overline{EI} & L/\overline{EI}
\end{bmatrix}
\begin{Bmatrix}
X_H \\[2mm]
X_V \\[2mm]
X_M
\end{Bmatrix}
\tag{3}
$$

2

Assuming both the support tube and the experiment housing to be constructed primarily of the same material, $\bar{E} = E$ and $\bar{\alpha} = \alpha$. The load matrix can now be isolated by grouping terms and factoring. Thus

$$
\begin{Bmatrix} X_H \\ X_V \\ X_M \end{Bmatrix} =
\begin{bmatrix}
\left(\dfrac{\bar{A}+A}{\bar{A}A} + \dfrac{\bar{h}^2}{4\bar{I}} + \dfrac{h^2}{4I}\right) & -\dfrac{L}{4}\left(\dfrac{\bar{h}}{\bar{I}} - \dfrac{h}{I}\right) & \dfrac{1}{2}\left(\dfrac{\bar{h}}{\bar{I}} - \dfrac{h}{I}\right) \\[2mm]
-\dfrac{L}{4}\left(\dfrac{\bar{h}}{\bar{I}} - \dfrac{h}{I}\right) & \dfrac{L^2}{3}\left(\dfrac{\bar{I}+I}{\bar{I}I}\right) & -\dfrac{L}{2}\left(\dfrac{\bar{I}+I}{\bar{I}I}\right) \\[2mm]
\dfrac{1}{2}\left(\dfrac{\bar{h}}{\bar{I}} - \dfrac{h}{I}\right) & -\dfrac{L}{2}\left(\dfrac{\bar{I}+I}{\bar{I}I}\right) & \left(\dfrac{\bar{I}+I}{\bar{I}I}\right)
\end{bmatrix}^{-1}
\begin{Bmatrix}
\alpha E\left[\bar{T} - T - \left(\dfrac{\overline{\Delta T} + \Delta T}{2}\right)\right] \\[2mm]
\dfrac{\alpha E L}{2}\left(\dfrac{\overline{\Delta T}}{\bar{h}} - \dfrac{\Delta T}{h}\right) \\[2mm]
-\alpha E\left(\dfrac{\overline{\Delta T}}{\bar{h}} \quad \dfrac{\Delta T}{h}\right)
\end{Bmatrix}
\qquad (4)
$$

A digital computer program written in Fortran II language for the solution of Equation (4) is listed in Appendix B as Program I. Using this program, interaction loads can be calculated for any number of cases. Loads for eight example cases were calculated and are listed in section A of the results.

Since optical alignments must be held within required limits, it is also of interest to obtain some estimate as to the amount of misalignment induced during flight conditions. The optical misalignment can be considered to be the relative angular displacement between two pre-aligned points. As shown in Figure 3, a single experiment is considered mounted symmetrically about the support tube midspan. The thermal gradients applied across the experiment and tube are assumed linear and constant over the length of both structures. Again the Euler-Bernoulli theory is assumed, but the experiment and tube are considered cantilevered at the tube midspan. It is also assumed that no relative rotations or displacements occur at the mounts.

Referring again to Figure 3 and selecting $\bar{P}'$ as a reference, the rotational deflection of $\bar{P}$ is simply the rotational terms for the hexagonal tube in Equation (2). Thus

$$
\delta_{\theta\bar{P}} = \frac{-\bar{\alpha}\overline{\Delta T}L}{\bar{h}} - \begin{bmatrix} 0 & -L^2/2\bar{E}\bar{I} & L/\bar{E}\bar{I} \end{bmatrix}
\begin{Bmatrix} X_H \\ X_V \\ X_M + X_H\dfrac{\bar{h}}{2} \end{Bmatrix}
\qquad (5)
$$

Expanding Equation (5) we get:

$$
\delta_{\theta\bar{P}} = \frac{-\bar{\alpha}\overline{\Delta T}L}{\bar{h}} + \frac{L^2 X_V}{2\bar{E}\bar{I}} - \frac{L X_M}{\bar{E}\bar{I}} - \frac{L\bar{h} X_H}{2\bar{E}\bar{I}}
$$

or

$$
\delta_{\theta\bar{P}} = \frac{-\bar{\alpha}\overline{\Delta T}L}{\bar{h}} + \frac{L}{\bar{E}\bar{I}}\left(\frac{L X_V}{2} - X_M - \frac{\bar{h} X_H}{2}\right)
\qquad (6)
$$

3

Since there are assumed no relative rotations or displacements at the mounts, Equation (6) also represents the rotational deflection of point P with respect to either $\bar{P}'$ or P'.

Next consider the rotational deflection of point $\bar{P}''$ at the left end of the support tube. If point $\bar{P}$ is selected as a reference, the rotational deflection of $\bar{P}''$ is due only to the temperature gradient across the tube. Therefore, if L is replaced by L' in the temperature induced rotational displacement term for the hexagonal tube in Equation (2), we get:

$$\delta_{\theta \bar{P}''/\bar{P}} = -\bar{a}\Delta\bar{T}L'/\bar{h} \tag{7}$$

The total rotational deflection of $\bar{P}''$ with respect to the midspan, P' or $\bar{P}'$, is equal to the algebraic sum of the relative deflections. Thus

$$\delta_{\theta \bar{P}''} = \delta_{\theta \bar{P}} + \delta_{\theta \bar{P}''/\bar{P}'} \tag{8}$$

Substituting for $\delta_{\theta \bar{P}}$ and $\delta_{\theta \bar{P}''/\bar{P}}$ and collecting terms

$$\delta_{\theta \bar{P}''} = \frac{-\bar{a}\Delta\bar{T}}{\bar{h}} (L + L') + \frac{L}{\overline{EI}} \left(\frac{LX_V}{2} - X_M - \frac{\bar{h}X_H}{2} \right) \tag{9}$$

Since the optical axis of the assumed experiment package has not been defined, the solutions of all three Equations (6), (7), and (9) may be of interest. A digital computer program written in Fortran II language for the solution of these three equations is listed in Appendix B as Program II. The program also yields the interaction loads introduced at points $\bar{P}$ and P, i.e., the solution of Equation (4).

RESULTS

A. Interaction Loads Introduced at the Forward Experiment Mount

Referring to Figure 1, the interaction loads introduced at points $\bar{P}$ and P were obtained through the solution of Equation (4) for the following eight cases:

Geometrical Properties Utilized

Hexagonal Tube	Experiment Housing (Assumed)
$\bar{I}$ = 28.03 in⁴ *	I = $\bar{I}/2$ and ∞, in⁴
$\bar{A}$ = 1.15 in²	A = 0.50 in²
$\bar{h}$ = 14 in	h = 7 in
$\bar{E}$ = 10⁷ psi	E = 10⁷ psi
$\bar{a}$ = 12.8 × 10⁻⁶ in/in/°F	a = 12.8 × 10⁻⁶ in/in/°F

*See Appendix C for calculations.

4

Temperature Distributions

(a)	(b)	(c)	(d)
$\Delta T = 0°F$	$\Delta T = 1°F$	$\Delta T = 0°F$	$\Delta T = 1°F$
$\overline{\Delta T} = 1°F$	$\overline{\Delta T} = 1°F$	$\overline{\Delta T} = 3°F$	$\overline{\Delta T} = 3°F$
$T = 0°F$	$T = 0°F$	$T = 0°F$	$T = 0°F$
$\overline{T} = 1°F$	$\overline{T} = 0°F$	$\overline{T} = 1°F$	$\overline{T} = 1°F$

Example Cases with Results

Case 1 - Assume $I = \overline{I}/2$, $L = 5.75$ in, and temperature distribution (a).

$X_H = 11.66$ lb

$X_V = 0.$ lb

$X_M = -85.45$ in-lb

Case 2 - Assume $I = \overline{I}/2$, $L = 28.5$ in, and temperature distribution (a).

$X_H = 11.66$ lb

$X_V = 0.$ lb

$X_M = -85.45$ in-lb

Case 3 - Assume $I = \overline{I}/2$, $L = 28.5$ in, and temperature distribution (b).

$X_H = -23.31$ lb

$X_V = 0.$ lb

$X_M = 85.46$ in-lb

Case 4 - Assume $I = \infty$, $L = 5.75$ in, and temperature distribution (a).

$X_H = 44.61$ lb

$X_V = 0.$ lb

$X_M = -568.52$ in-lb

Case 5 - Assume $I = \infty$, $L = 28.5$ in, and temperature distribution (a).

$X_H = 44.61$ lb

$X_V = 0.$ lb

$X_M = -568.52$ in-lb

Case 6 - Assume $I = \infty$, $L = 28.5$ in, and temperature distribution (b).

$X_H = -66.91$ lb

$X_V = 0.$ lb

$X_M = 724.64$ in-lb

Case 7 - Assume $I = \overline{I}/2$, $L = 28.5$ in, and temperature distribution (c).

$X_H = -11.65$ lb

$X_V = 0.$ lb

$X_M = -256.33$ in-lb

Case 8 - Assume $I = \infty$, $L = 28.5$ in, and temperature distribution (d).

$X_H = -22.30$ lb.

$X_V = 0.$ lb

$X_M = -100.15$ in-lb

It is of interest to note that the vertical force, X_V, is equal to zero for all eight cases. For the assumed configuration, the vertical force, X_V, is always zero. This relation is shown in Appendix A.

B. Induced Rotational Deflections

Equations (6), (7), and (9) were solved for the configuration depicted in Figure 3. The first run utilized the fillowing input values assuming aluminum alloy for both the experiment housing and the hexagonal tube: $\overline{I} = 28.03$ in^4, $I = \overline{I}/8$, $\overline{A} = 1.15$ in^2, $A = 0.50$ in^2, $\overline{h} = 14$ in, $h = 7$ in, $E = 10^7$ psi, $\alpha = 12.8 \times 10^{-6}$ in/in/°F, $L = 10.51$ in, and $L' = 16.17$ in. A total of 144 different cases of temperature-gradient combinations were considered. In many instances, the same deflection resulted for different temperature-gradient combinations. Therefore, cases yielding like deflections were grouped together where each group number identifies the first case in that particular group. These groups are listed in Table I along with the corresponding temperature-gradient values for each case.

The results are presented as sets of parametric curves for the various groups in Figures 4, 5, and 6 with deflections plotted as a function of the temperature gradient across the hexagonal tube. Figure 4 shows the variation of $\delta_{\theta\overline{P}}$ with $\overline{\Delta T}$. This deflection is represented in Program II by the variable name, DEFHEX (see Appendix B). Since the curve slopes are equal and constant for all groups, the effect of changing the temperature-gradient combinations is to shift the curve along the ordinate to a new deflection for a given $\overline{\Delta T}$ reference. This shows that for a given deflection there exists a range of possible $\overline{\Delta T}$'s. It is of interest to note that zero deflections are theoretically possible for $\overline{\Delta T}$'s in the range of ± 7 seconds of arc. The apparent subgroups of three are for cases containing similar T and $\overline{T}$ parameters. The variable within these subgroups is the less significant ΔT parameter. The single curve in Figure 5 indicates the variation of $\delta_{\theta\overline{P}''/\overline{P}}$ with $\overline{\Delta T}$ for all groups since, from Equation (7), the free bending of the beam is dependent only on the thermal variable, $\overline{\Delta T}$, holding α, L', and $\overline{h}$ constant. This deflection is denoted by the variable name DEFREL in Program II. The slope of this function is shown to be -3.051 arc sec/°F. The variation of $\delta_{\theta\overline{P}''}$ with $\overline{\Delta T}$ is shown in Figure 6. This deflection is the algebraic sum of DEFHEX and DEFREL and has the variable name DEFEND in Program II. As indicated, zero deflections are also theoretically possible for $\overline{\Delta T}$'s in the range of ± 7 seconds of arc. The slope of these curves is shown to be -3.845 arc sec/°F.

Several additional runs were executed varying such parameters as the type of structural material, length of support tube, distance between experiment mounts, and experiment housing cross sectional moment of inertia. In addition, runs were executed for zero and exceptionally large temperature gradients across the experiment housing. Parameters for all runs are listed in Table II.

Group I was selected as the criterion for correlating the results in the several runs. These results are indicated in Table III and Figures 7 and 8. Table III includes the slope $\Delta\delta_{\theta\overline{P}}/\Delta(\overline{\Delta T})$ and the corresponding interaction loads for the respective runs. The longitudinal interaction force, X_H, and interaction moment, X_M, are shown respectively in Figures 7 and 8 for each run. The

results indicate that run 4 with Beryllium as the structural material yields the lowest deflection for a given transverse temperature gradient, $\overline{\Delta T}$. This run also lends itself to the highest interaction loads as might be expected. Comparing runs 1 and 2, the effect of zero thermal gradient across the experiment housing is to decrease the horizontal force, X_H, by approximately 3% and increase the moment, X_M, by about 13%. However, as displayed in run 3, a ΔT of 7°F greatly reduces X_M by about 80% while increasing X_H by approximately 20%. It is of interest to observe that the deflection curve slope is not affected appreciably by changes in ΔT in the range considered i.e., 0 - 13°F. Considering runs 1 and 6, it is seen that increasing the experiment housing cross sectional moment of inertia by a factor of ten increases X_M by approximately 37%, decreases X_H by about 6%, and, most significantly, reduces the deflection slope by approximately 31%. Doubling the support tube length or, more meaningful, increasing the distance between experiment mounting points (run 5) yields a change in the deflection slope which is indicated to be directly proportional to this ΔL. This relation is seen by dividing Equation (6) by $\overline{\Delta T}$ and recalling that X_V equals zero. An interesting result in comparing runs 1 and 5 is that the interaction loads are not a function of L. This result can be shown by expanding Equation (4). This expansion also shows the vertical load, X_V, to be zero as indicated in Appendix A.

CONCLUDING REMARKS

For the mathematical model of one experiment combined with the support tube under the indicated assumptions, the following points may be concluded from the results.

1. It is possible to obtain the same misalignment or rotational deflection for different combinations of T, $\overline{T}$, and ΔT.

2. It is possible to maintain zero deflection for $\overline{\Delta T}$ in the range of ±7°F if the values of T, $\overline{T}$ and ΔT are properly chosen.

3. Changes in T and $\overline{T}$ are more significant to misalignment than changes in ΔT.

4. The rotational deflection is directly proportional to L.

5. The interaction loads are independent of changes in L.

References

1. McMinn, S. J.: "Matrices for Structural Analysis," John Wiley and Sons, Inc., New York, 1962.

2. "Design Study of AOSO RAC-762-5-I Tech. Vol. I," Republic Aviation Corp., Long Island, New York, 1962.

3. "Honeycomb Sandwich Design," Brochure "E," Hexcel Products Inc.

4. Hoff, N. J., and Mautner, S. E., "Bending and Buckling of Sandwich Beams," Journal of the Aeronautical Sciences, Vol. 15, No. 12, pp. 707-720, December 1948.
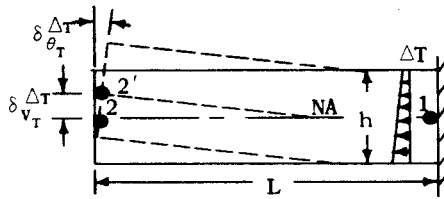
APPENDIX A

I. DEVELOPMENT OF INDIVIDUAL TERMS WITH EQUATION (2)

A. Temperature induced displacement and rotation matrices

$$\{\delta_T\} \equiv \begin{Bmatrix} \delta_{H_T} \\ \delta_{V_T} \\ \delta_{\theta_T} \end{Bmatrix} \tag{A.1}$$
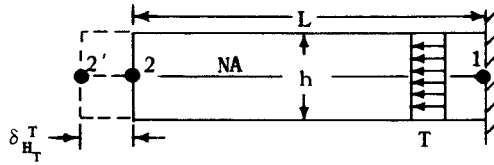
Sketch A-1
Displacements due to a uniform
temperature increase.

Sketch A-2
Displacements due to a linear vertical
temperature gradient.

From Sketches A-1 and A-2, induced displacements at point (2) relative to point (1) due to a uniform temperature increase (T) and a linear vertical temperature gradient (ΔT) are shown respectively to be

$$\delta_{H_T}^T = \alpha T L \ , \qquad \delta_{V_T}^T = \delta_{\theta_T}^T = 0 \tag{A.2}$$

and

$$\delta_{H_T}^{\Delta T} = 0* , \qquad \delta_{V_T}^{\Delta T} = \frac{\alpha \Delta T L^2}{2h} , \qquad \delta_{\theta_T}^{\Delta T} = -\frac{\alpha \Delta T L}{h} \tag{A.3}$$

*Assuming small deflections.

9

The induced displacements of point (P) relative to point (1) can be expressed as

$$\delta_{H_T} = \delta_{H_T}^T + \left(\delta_{\theta_T}^T\right)\frac{h}{2} = \alpha TL + \frac{\alpha\Delta TL}{2} \tag{A.4a}$$

$$\delta_{V_T} = \delta_{V_T}^T + \delta_{V_T}^{\Delta T} = 0 + \frac{\alpha\Delta TL^2}{2h} \tag{A.4b}$$

$$\delta_{\theta_T} = \delta_{\theta_T}^T + \delta_{\theta_T}^{\Delta T} = 0 - \frac{\alpha\Delta TL}{h} \tag{A.4c}$$

Therefore, Equation (A.1) becomes

$$\{\delta_T\} = \left\{\begin{array}{c} \alpha L\left(T + \dfrac{\Delta T}{2}\right) \\[2ex] \dfrac{\alpha\Delta TL^2}{2h} \\[2ex] \dfrac{-\alpha\Delta TL}{h} \end{array}\right\} \tag{A.5}$$
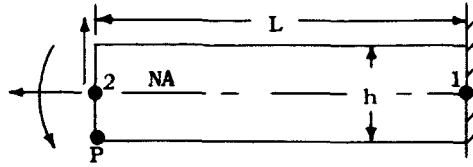
Going through a similar development, it can be shown that for point ($\bar{P}$) relative to point (3),

$$\{\bar{\delta}_T\} = \left\{\begin{array}{c} \bar{\alpha}L\left(\bar{T} - \dfrac{\overline{\Delta T}}{2}\right) \\[2ex] \dfrac{\bar{\alpha}\overline{\Delta T}L^2}{2\bar{h}} \\[2ex] \dfrac{-\bar{\alpha}\overline{\Delta T}L}{\bar{h}} \end{array}\right\} \tag{A.6}$$

B. Influence coefficient matrix for loads applied at the neutral axis

$$[f] = \begin{bmatrix} f_{HH} & f_{VH} & f_{\theta H} \\[2ex] f_{HV} & f_{VV} & f_{\theta V} \\[2ex] f_{H\theta} & f_{V\theta} & f_{\theta\theta} \end{bmatrix} \tag{A.7}$$

10

Where f_{ij} is defined as the displacement in the j direction due to a load applied in the i direction

Sketch A-3
Unit loads applied at the
neutral axis, point (2).

For unit loads applied at point (2), see Sketch (A-3), terms in Equation (A.7) for displacements at point (2) become

$$f_{HH} = \frac{L}{AE} \qquad f_{VH} = 0 \qquad f_{\theta H} = 0$$

$$f_{HV} = 0 \qquad f_{VV} = \frac{L^3}{3EI} \qquad f_{\theta V} = \frac{-L^2}{2EI}$$

$$f_{H\theta} = 0 \qquad f_{V\theta} = \frac{-L^2}{2EI} \qquad f_{\theta\theta} = \frac{L}{EI}$$

Therefore, for displacements at point (2) due to unit loads at point (2), Equation (A.7) becomes

$$[f] = \begin{bmatrix} \dfrac{L}{AE} & 0 & 0 \\[2ex] 0 & \dfrac{L^3}{3EI} & \dfrac{-L^2}{2EI} \\[2ex] 0 & \dfrac{-L^2}{3EI} & \dfrac{L}{EI} \end{bmatrix} \qquad\qquad (A.8)$$

Considering displacements at point (P) due to unit loads applied at point (2) as shown in Sketch (A-3), the following two changes occur in the individual terms of Equation (A.8):

$$f_{VH} = \left(f_{V\theta}\right)\frac{h}{2} = \frac{L^2 h}{4EI}$$

$$f_{\theta H} = \left(f_{\theta\theta}\right)\frac{h}{2} = \frac{-Lh}{2EI}$$

11

Therefore, the influence matrix of Point (P) for loads applied at point (2) (neutral axis) becomes

$$[f] = \begin{bmatrix} \dfrac{L}{AE} & \dfrac{L^2 h}{4EI} & \dfrac{-Lh}{2EI} \\[2em] 0 & \dfrac{L^3}{3EI} & \dfrac{-L^2}{2EI} \\[2em] 0 & \dfrac{-L^2}{2EI} & \dfrac{L}{EI} \end{bmatrix} \qquad (A.9)$$

Using a similar development, it can be shown that the influence matrix of Point ($\bar{P}$) (see Figure 2) for loads applied at point (4) (neutral axis) becomes

$$[\bar{f}] = \begin{bmatrix} \dfrac{L}{\overline{AE}} & \dfrac{-L^2 \bar{h}}{4\overline{EI}} & \dfrac{L\bar{h}}{2\overline{EI}} \\[2em] 0 & \dfrac{L^3}{3\overline{EI}} & \dfrac{-L^2}{2\overline{EI}} \\[2em] 0 & \dfrac{-L^2}{2\overline{EI}} & \dfrac{L}{\overline{EI}} \end{bmatrix} \qquad (A.10)$$

C. Off neutral axis load matrix referenced to neutral axis

$$\{X\} \equiv \begin{Bmatrix} X_H \\ X_V \\ X_M \end{Bmatrix} \qquad (A.11)$$
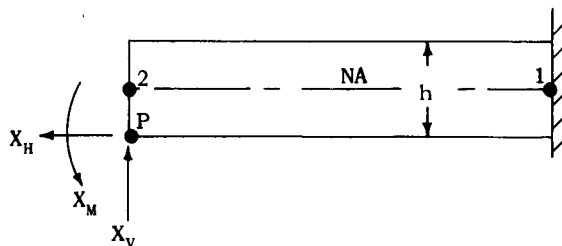
Sketch A-4
Unit loads applied at point
(P) off neutral axis.

With reference to Sketch (A-4), the indicated loads applied at point (P) reflect the following loads at point (2):

$$X_H = {}^P X_H$$

$$X_V = {}^P X_V$$

$$X_M = {}^P X_M - {}^P X_H \frac{h}{2}$$

Substituting these expressions into Equation (A.11) and dropping the pre-superscript (P) yields the following load matrix at point (2) (neutral axis) due to off axis applied loads (point (P)):

$$\{X\} = \left\{ \begin{array}{c} X_H \\ X_V \\ X_M - X_H \dfrac{h}{2} \end{array} \right\} \tag{A.12}$$

Similarly, for loads applied at point $(\bar{P})$ (see Figure 2) referenced to the neutral axis, point (4)

$$\{\bar{X}\} = \left\{ \begin{array}{c} X_H \\ X_V \\ X_M + X_H \dfrac{\bar{h}}{2} \end{array} \right\} \tag{A.13}$$

II.   IDENTITY FOR VERTICAL LOAD, X_V

In Part A of the results it was first shown that, for the assumed configuration, the vertical force, X_V, is always zero. This result can be shown as follows: Writing Equation (4) in contracted form as

$$\{X\} = [f + \bar{f}]^{-1} \{\delta_T + \bar{\delta}_T\} \tag{A.14}$$

and redefining the inverse of the combined influence coefficient matrix as

$$[f + \bar{f}]^{-1} = [F]^{-1} \equiv [k] \tag{A.15}$$

13

and the combined temperature induced displacement and rotation matrix as

$$\{\delta_T + \bar{\delta}_T\} \equiv \{d\}$$ (A.16)

Equation (4) can be also expressed in contracted form as

$$\{x\} = [k]\{d\}$$ (A.17)

$[k]$ is known as the combined stiffness matrix. Expanding Equation (A.17) yields

$$\begin{Bmatrix} X_H \\ X_V \\ X_\theta \end{Bmatrix} = \begin{bmatrix} k_{11} & k_{12} & k_{13} \\ k_{21} & k_{22} & k_{23} \\ k_{31} & k_{32} & k_{33} \end{bmatrix} \begin{Bmatrix} d_1 \\ d_2 \\ d_3 \end{Bmatrix}$$ (A.18)

Solving for X_V

$$X_V = k_{21} d_1 + k_{22} d_2 + k_{23} d_3$$ (A.19)

Where k_{21}, k_{22} and k_{23} are the second row terms of $[F]^{-1}$ in Equation (A.15).

The inverse of $[F]$ is equal to the adjoint of $[F]$ divided by the determinant of $[F]$. Since $[F]$ is symmetrical, the transpose of $[F]$ equals $[F]$. Further, the adjoint of $[F]$ becomes just the cofactor of $[F]$. Therefore, Equation (A.19) can be expressed in the form

$$X_V = \frac{C_{21}}{|F|} d_1 + \frac{C_{22}}{|F|} d_2 + \frac{C_{23}}{|F|} d_3$$ (A.20)

where C_{ij} are the cofactors of the F_{ij} terms of $[F]$, and $|F|$ is the determinant of $[F]$.

Expanding the second row cofactors of $[F]$

$$C_{21} = -(F_{12} F_{33} - F_{13} F_{32}) ; \qquad C_{22} = +(F_{11} F_{33} + F_{13} F_{31}) ;$$

$$C_{23} = -(F_{11} F_{32} - F_{12} F_{31})$$

Substituting into Equation (A.20) yields

$$X_V = \frac{1}{|F|} \left\{ (-F_{12} F_{33} + F_{13} F_{32}) d_1 + (F_{11} F_{33} - F_{13} F_{31}) d_2 + (-F_{11} F_{32} + F_{12} F_{31}) d_3 \right\}$$ (A.21)

14

Substituting terms of Equation (4) into Equation (A.21)

$$X_v = \frac{1}{|F|} \left\{ \left[\frac{L}{4} \left(\frac{\bar{h}}{\bar{I}} - \frac{h}{I} \right) \left(\frac{\bar{I} + I}{\bar{I}I} \right) - \frac{L}{4} \left(\frac{\bar{h}}{\bar{I}} - \frac{h}{I} \right) \left(\frac{\bar{I} + I}{\bar{I}I} \right) \right] \left[\alpha E (\bar{T} - T) \right] \right.$$

$$+ \left[\left(\frac{\bar{A} + A}{\bar{A}A} + \frac{\bar{h}^2}{4\bar{I}} + \frac{h^2}{4I} \right) \left(\frac{\bar{I} + I}{\bar{I}I} \right) - \frac{1}{4} \left(\frac{\bar{h}}{\bar{I}} - \frac{h}{I} \right)^2 \right] \left[\frac{\alpha EL}{2} \left(\frac{\overline{\Delta T}}{\bar{h}} - \frac{\Delta T}{h} \right) \right]$$

$$- \left. \left[\frac{L}{2} \left(\frac{\bar{A} + A}{\bar{A}A} + \frac{\bar{h}^2}{4\bar{I}} + \frac{h^2}{4I} \right) - \frac{L}{8} \left(\frac{\bar{h}}{\bar{I}} - \frac{h}{I} \right)^2 \right] \left[\alpha E \left(\frac{\overline{\Delta T}}{\bar{h}} - \frac{\Delta T}{h} \right) \right] \right\} \text{(A.22)}$$

Since $C_{21} d_1 = 0$ and $C_{22} d_2 = -C_{23} d_3$,

$$X_v = 0 \tag{A.23}$$

for all cases.

15

APPENDIX B

Fortran Listing of Programs I and II

I. SYMBOL INTERPRETATION

Fortran	Problem
A	A
AH	h
AI	I
AL	L
DT	$\triangle T$
DTB	$\overline{\triangle T}$
T	T
TB	$\overline{T}$
EE	E
ALPHA	α
AIB	$\overline{I}$
AHB	$\overline{h}$
AB	$\overline{A}$
Z(ij)	$(f + \overline{f})_{ij}$
C(ij)	Cofactor of $(f + \overline{f})_{ij}$
D	Determinant of $\left[f + \overline{f}\right]$

II. LISTING OF PROGRAM I

```
C          PROGRAM I
           DIMENSION Z(50), C(50), F(10)
10 FORMAT (8F9.4)
11 FORMAT (F10.2)
12 FORMAT (3(1PE15.4))
13 FORMAT (8E15.4)
14 FORMAT (6E20.5)
15 FORMAT (9E15.5)
16 FORMAT (1H0)
 1 READ INPUT TAPE 2, 10, A, AH, AI, AL, BT, BTU, T, TU, EE, ALPHA,
  $AIE, AHE, AE
   WRITE OUTPUT TAPE 3, 13, A, AH, AI, AL, BT, BTU, T, TU, EE, ALPHA,
  $AIE, AHE, AE
   Z(11) = (AU+A)/(AL*A)+AHE**2/(4.*AIE)+AH**2/(4.*AI)
   Z(12) = -AL/4.*(AHE/AIE-AH/AI)
   Z(13) = .5*(AHE/AIE-AH/AI)
   Z(33) = (AIU+AI)/(AIE*AI)
   Z(22) = AL**2/3.*Z(33)
   Z(23) = -AL/2.*Z(33)
   Z(21) = Z(12)
   Z(31) = Z(13)
   Z(32) = Z(23)
   C(11) = Z(22)*Z(33)-Z(23)*Z(32)
   C(12) =-Z(21)*Z(33)+Z(23)*Z(31)
   C(13) = Z(21)*Z(32)-Z(22)*Z(31)
   C(21) =-Z(12)*Z(33)+Z(13)*Z(32)
   C(22) = Z(11)*Z(33)-Z(13)*Z(31)
   C(23) =-Z(11)*Z(32)+Z(12)*Z(31)
   C(31) = Z(12)*Z(23)-Z(13)*Z(22)
   C(32) =-Z(11)*Z(23)+Z(13)*Z(21)
   C(33) = Z(11)*Z(22)-Z(12)*Z(21)
   D = Z(11)*Z(22)*Z(33)+Z(12)*Z(23)*Z(31)+Z(13)*Z(32)*Z(21)
  $  -Z(13)*Z(22)*Z(31)-Z(12)*Z(21)*Z(33)-Z(11)*Z(32)*Z(23)
   Y = EE*ALPHA/D
   Z(01) = (TU-T-(BTU+BT)/2.)*AI
   Z(02) = AL/2.*(BTU/AHE-BT/AH)*Y
   Z(03) = (-BTU/AHE+BT/AH)*Y
   DO 5 I=1,3
   IX = 10*I+1
   IY = 10*I+2
   IZ = 10*I+3
   F(I) = C(IX)*Z(01)+C(IY)*Z(02)+C(IZ)*Z(03)
 5 WRITE OUTPUT TAPE 3, 11, F(I)
   DEFHEX = (-ALPHA*BTU*AL/AHE+AL**2*F(2)/(2.*EE*AIE)-AL/(EE*AIE)*
  $  (F(3)+F(1)*AHE/2.))*2.00000E5
   DEFLXP = (-ALPHA*BT*AL/AH-AL**2*F(2)/(2.*EE*AI)+AL/(EE*AI)*
  $  (F(3)-F(1)*AH/2.))*2.00000E5
   WRITE OUTPUT TAPE 3, 12, DEFHEX, DEFLXP
   WRITE OUTPUT TAPE 3, 16
   GO TO 1
   END
```

18

III. LISTING OF PROGRAM II

```
C         PROGRAM II
          DIMENSION Z(50), C(50), F(10)
   10 FORMAT (5E14.4)
   11 FORMAT (1H0,4X,5HX(H)=F10.4/5X,5HX(V)=10.4/5X,5HX(M)=F10.4/)
   12 FORMAT (10E12.4)
   13 FORMAT (1H0)
   14 FORMAT (7F15.6,10X,4HCASEI4)
   15 FORMAT (45X,10HDATA INPUT)
   16 FORMAT (1H0,50X,7HRESULTS)
   17 FORMAT (1H0,6X,1HA,11X,1HH,10X,1HE,10X,5HALPHA,6X,3H1 BAR,7X,
      55HH BAR,7X,5HA BAR,9X,1HI,10X,1HL,10X,2HL2)
   18 FORMAT (1H0,7X,7HDELTA T,12X,1HT,12X,5HT BAR,7X,1HDELTA T BAR,6X,
      56HDEFHEX,6X,6HDEFREL,9X,6HDEFEND)
    1 READ INPUT TAPE 2,10, A, AH, EE, ALPHA, AIB, AHB, AB, AI, AL, AL2
      WRITE OUTPUT TAPE 3,15
      WRITE OUTPUT TAPE 3,17
      WRITE OUTPUT TAPE 3,12, A, AH, EE, ALPHA, AIB, AHB, AB, AI, AL,AL2
      WRITE OUTPUT TAPE 3,16
      ICASE = 1
      DO 20 J=1,5,2
      DT=J
      KSIGN=1
    8 DO 45 K=1,13,4
      T=K*KSIGN
      LSIGN=1
    9 DO 35 L=1,5,2
      TB=L*LSIGN
      MSIGN=1
    7 DO 25 M=7,7,6
      DTB=M*MSIGN
      Z(11) = (AB+AI)/(AB*AI)+AHB**2/(4.*AIB)+AH**2/(4.*AI)
      Z(12) = -AL/4.*(AHB/AIB-AH/AI)
      Z(13) = .5*(AHB/AIB-AH/AI)
      Z(33) = (AIB+AI)/(AIB*AI)
      Z(22) = AL**2/3.*Z(33)
      Z(23) = -AL/2.*Z(33)
      Z(21) = Z(12)
      Z(31) = Z(13)
      Z(32) = Z(23)
      C(11) = Z(22)*Z(33)-Z(23)*Z(32)
      C(12) =-Z(21)*Z(33)+Z(23)*Z(31)
      C(13) = Z(21)*Z(32)-Z(22)*Z(31)
      C(21) =-Z(12)*Z(33)+Z(13)*Z(32)
      C(22) = Z(11)*Z(33)-Z(13)*Z(31)
      C(23) =-Z(11)*Z(32)+Z(12)*Z(31)
      C(31) = Z(12)*Z(23)-Z(13)*Z(22)
      C(32) =-Z(11)*Z(23)+Z(13)*Z(21)
      C(33) = Z(11)*Z(22)-Z(12)*Z(21)
      D = Z(11)*Z(22)*Z(33)+Z(12)*Z(23)*Z(31)+Z(13)*Z(32)*Z(21)
      5   -Z(13)*Z(22)*Z(31)-Z(12)*Z(21)*Z(33)-Z(11)*Z(32)*Z(23)
      Y = EE*ALPHA/D
      Z(01) = (TB-T-(DTB+DT)/2.)*Y
```

```
      Z(02) = AL/2.*(DTB/AHB-DT/AH)*Y
      Z(03) = (-DTB/AHB+DT/AH)*Y
      DO 5 I=1,3
      IX = 10*I+1
      IY = 10*I+2
      IZ = 10*I+3
    5 F(I) = C(IX)*Z(01)+C(IY)*Z(02)+C(IZ)*Z(03)
      WRITE OUTPUT TAPE 3, 11,(F(I),I=1,3)
      WRITE OUTPUT TAPE 3,18

      DEFHEX = (-ALPHA*DTB*AL/AHB+AL**2*F(2)/(2.*EE*AIB)-AL/(EE*AIB)*
     $  (F(3)+F(1)*AHB/2.))*2.0636E5
      DEFREL=-ALPHA*DTB*AL2*2.0636E5/AHB
      DEFEND= DEFHEX+DEFREL
      WRITE OUTPUT TAPE 3,14, DT, T, TB, DTB, DEFHEX, DEFREL, DEFEND,
     $ICASE
   25 CONTINUE
      IF(MSIGN) 34,30,26
   26 MSIGN=-1
      GO TO 7
   34 ICASE = ICASE + 1
   35 CONTINUE
      IF(LSIGN) 45,30,36
   36 LSIGN=-1
      GO TO 9
   45 CONTINUE
      IF(KSIGN) 20,30,46
   46 KSIGN=-1
      GO TO 8
   30 CALL DUMP
   20 CONTINUE
      GO TO 1
      END
```

APPENDIX C

Moment of Inertia Calculation for the Proposed Honeycomb Sandwhich Hexagonal Tube
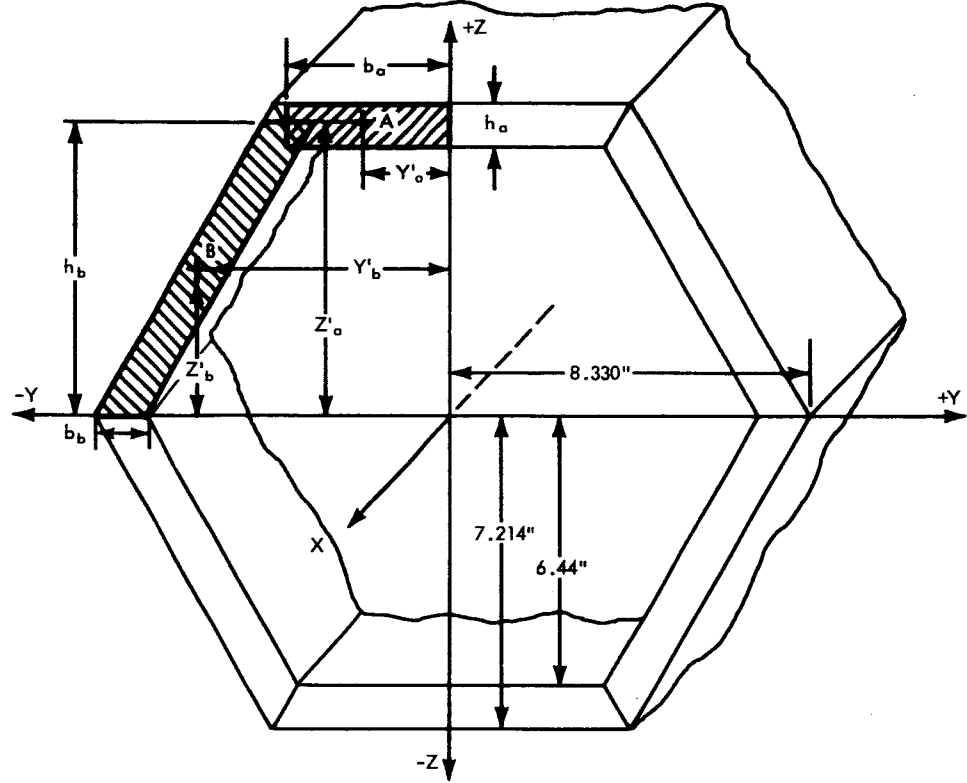
Sketch C-1

As indicated in Sketch C-1, the proposed support tube is composed of six honeycomb sandwich beams joined to form a symmetrical hexagonal cross section. Considering a typical cross section of the honeycomb sandwich structure as shown in Sketch C-2, the moment of inertia about its y-y axis can be expressed as
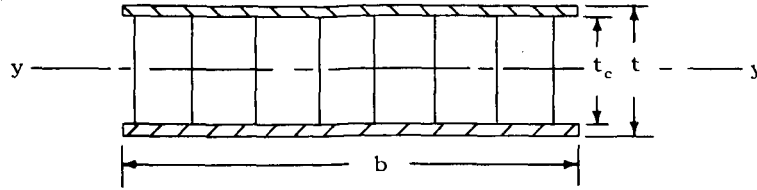
$$I_y = \frac{b\left(t^3 - t_c^3\right)}{12} \tag{C.1}$$

where

    t Sandwich thickness

    t_c Core thickness

    b Section width

Sketch C-2

Since the cross section of the tube is symmetrical across both the Y and Z axes, only one quadrant need be calculated and then multiplied by four to obtain the total cross sectional inertia of the tube about the Y-Y axis.

Referring again to sketch C-1, the -Y/-Z quadrant is shown to be subdivided into two sections, A and B. Expressing the total inertia of the tube in terms of these two sections

$$I_Y = 4 \sum_{i=a}^{b} \left[\overline{I}_{yi} + (Z_i')^2 A_i \right] \tag{C.2}$$
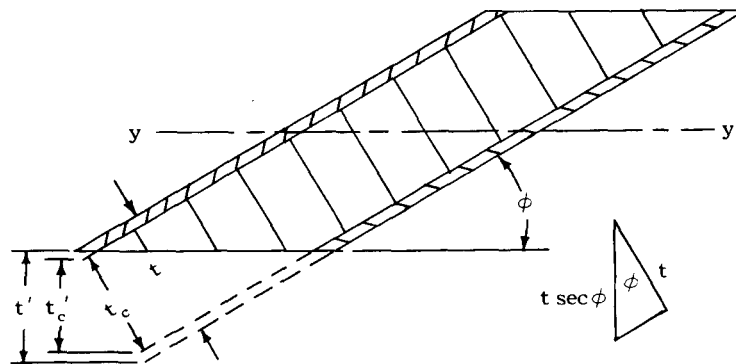
where

$\overline{I}_{yi}$ Centrodial area inertia about the y-y axis of section i

Z_i' Normal distance from Y-Y axis to centrodial (y-y) axis of section i

A_i Effective cross sectional area of section i

Expanding Equation (C.2)

$$I_Y = 4 \left[\overline{I}_{ya} + (Z_a')^2 A_a + \overline{I}_{yb} + (Z_b')^2 A_b \right] \tag{C.3}$$

Sketch C-3

22

With reference to Equation (C.1) and Sketches (C-2) and (C-3), the centrodial area inertias for sections A and B can be expressed respectively as

$$\overline{I}_{ya} = \frac{b_a}{12} \left(t^3 - t_c^3 \right) \tag{C.4}$$

$$\overline{I}_{yb} = \frac{b_b}{12} \left[(t')^3 - (t_c')^3 \right] \tag{C.5}$$

From Sketch C-3, t' and t_c' can be expressed in terms of t and t_c as

$$t' = t \sec \phi \tag{C.6a}$$

and

$$t_c' = t_c \sec \phi \tag{C.6b}$$

Substituting Equations (C.6) into Equation (C.5)

$$\overline{I}_{yb} = \frac{b_b \sec^3 \phi}{12} \left(t^3 - t_c^3 \right) \tag{C.7}$$

Assuming the effective area for bending to be only the face sheet cross section of the sandwich structure, the effective areas become (see Sketch C-1)

$$A_a = b_a \left(t - t_c \right) \tag{C.8a}$$

$$A_b = 2 A_a \tag{C.8b}$$

Substituting Equations (C.4), (C.7), (C.8a) and (C.8b) into Equation (C.3)

$$I_Y = 4 \left\{ b_a \left[\frac{\left(t^3 - t_c^3 \right)}{12} + (Z_a')^2 \left(t - t_c \right) \right] \right.$$

$$\left. + \frac{b_b \sec^3 \phi}{12} \left(t^3 - t_c^3 \right) + 2 (Z_b')^2 b_a \left(t - t_c \right) \right\} \tag{C.9}$$

The following values for parameters in Equation (C.9) were used to evaluate I_y.

$$t = 0.774 \text{ in.}$$

$$t_c = 0.750 \text{ in.}$$

$$b_a = 4.165 \text{ in.}$$

$$b_b = 0.894 \text{ in.}$$

$$Z_a' = 6.827 \text{ in.}$$

$$Z_b' = 3.413 \text{ in.}$$

$$\phi = 30°$$

Solving Equation (C.9) for these values yields an I_y equal to 28.03 in^4.

Table I

Grouped Run Cases with Thermal Parameters.

Group No	Case No	ΔT T T̄	Group No	Case No	ΔT T T̄	Group No	Case No	ΔT T T̄
1	1	1 1 1	49	49	3 1 1	97	97	5 1 1
	9	1 5 5		57	3 5 5		105	5 5 5
	28	1 -1 -1		76	3 -1 -1		124	5 -1 -1
	36	1 -5 -5		84	3 -5 -5		132	5 -5 -5
2	2	1 1 3	50	50	3 1 3	98	98	5 1 3
	25	1 -1 1		73	3 -1 1		121	5 -1 1
	35	1 -5 -3		83	3 -5 -3		131	5 -5 -3
3	3	1 1 5	51	51	3 1 5	99	99	5 1 5
	26	1 -1 3		74	3 -1 3		122	5 -1 3
	34	1 -5 -1		82	3 -5 -1		130	5 -5 -1
	42	1 -9 -5		90	3 -9 -5		138	5 -9 -5
4	4	1 1 -1	52	52	3 1 -1	100	100	5 1 -1
	8	1 5 3		56	3 5 3		104	5 5 3
	29	1 -1 -3		77	3 -1 -3		125	5 -1 -3
5	5	1 1 -3	53	53	3 1 -3	101	101	5 1 -3
	7	1 5 1		55	3 5 1		103	5 5 1
	15	1 9 5		63	3 9 5		111	5 9 5
	30	1 -1 -5		78	3 -1 -5		126	5 -1 -5
6	6	1 1 -5	54	54	3 1 -5	102	102	5 1 -5
	10	1 5 -1		58	3 5 -1		106	5 5 -1
	14	1 9 3		62	3 9 3		110	5 9 3
11	11	1 5 -3	59	59	3 5 -3	107	107	5 5 -3
	13	1 9 1		61	3 9 1		109	5 9 1
	21	1 13 5		69	3 13 5		117	5 13 5
12	12	1 5 -5	60	60	3 5 -5	108	108	5 5 -5
	16	1 9 -1		64	3 9 -1		112	5 9 -1
	20	1 13 3		68	3 13 3		116	5 13 3
17	17	1 9 -3	65	65	3 9 -3	113	113	5 9 -3
	19	1 13 1		67	3 13 1		115	5 13 1
18	18	1 9 -5	66	66	3 9 -5	114	114	5 9 -5
	22	1 13 -1		70	3 13 -1		118	5 13 -1
23	23	1 13 -3	71	71	3 13 -3	119	119	5 13 -3
24	24	1 13 -5	72	72	3 13 -5	120	120	5 13 -5
27	27	1 -1 5	75	75	3 -1 5	123	123	5 -1 5
	31	1 -5 1		79	3 -5 1		127	5 -5 1
	41	1 -9 -3		89	3 -9 -3		137	5 -9 -3
32	32	1 -5 3	80	80	3 -5 3	128	128	5 -5 3
	40	1 -9 -1		88	3 -9 -1		136	5 -9 -1
	48	1 -13 -5		96	3 -13 -5		144	5 -13 -5
33	33	1 -5 5	81	81	3 -5 5	129	129	5 -5 5
	37	1 -9 1		85	3 -9 1		133	5 -9 1
	47	1 -13 -3		95	3 -13 -3		143	5 -13 -3
38	38	1 -9 3	86	86	3 -9 3	134	134	5 -9 3
	46	1 -13 -1		94	3 -13 -1		142	5 -13 -1
39	39	1 -9 5	87	87	3 -9 5	135	135	5 -9 5
	43	1 -13 1		91	3 -13 1		139	5 -13 1
44	44	1 -13 3	92	92	3 -13 3	140	140	5 -13 3
45	45	1 -13 5	93	93	3 -13 5	141	141	5 -13 5

Table II

Parameters for Program II Runs.

Run No.	Material	α (in/in/°F)	E psi	Support Tube Length (in)	L (in)	L' (in)	I (in⁴)	$\bar{I}$ (in⁴)	ΔT(°F) Range	h (in)	$\bar{h}$ (in)	A (in²)	$\bar{A}$ (in²)
1	Aluminum	12.8×10^{-6}	10^7	60	10.51	16.17	3.514	28.03	1 - 5	7	14	0.5	1.2
2	Aluminum	12.8×10^{-6}	10^7	60	10.51	16.17	3.514	28.03	0	7	14	0.5	1.2
3	Aluminum	12.8×10^{-6}	10^7	60	10.51	16.17	3.514	28.03	7 - 13	7	14	0.5	1.2
4	Beryllium	7.39×10^{-6}	4.2×10^7	60	10.51	16.17	3.514	28.03	1 - 5	7	14	0.5	1.2
5	Aluminum	12.8×10^{-6}	10^7	120	48.00	12.00	3.514	28.03	1 - 5	7	14	0.5	1.2
6	Aluminum	12.8×10^{-6}	10^7	60	10.51	16.17	35.14	28.03	1 - 5	7	14	0.5	1.2

Table III

Deflection Curve Slopes and Interaction Loads for Program II Runs.

Run No	Case No	$\overline{\Delta T}$(°F)	ΔT(°F)	Slope* (Arc Sec/°F)	X_H(lb)	X_M(in-lb)
1	1	+7	+1	-0.794	- 97.18	-369.21
2	1	+7	0	-0.794	- 93.82	-418.47
3	1	+7	+7	-0.794	-117.34	- 73.61
4	1	+7	+1	-0.455	-237.00	-898.41
5	1	+7	+1	-3.628	- 97.18	-369.21
6	1	+7	+1	-0.547	- 87.76	-507.37

*Slope = $\Delta \delta_{\theta \overline{P}} / \Delta(\overline{\Delta T})$ or DEFHEX/$\Delta(\overline{\Delta T})$
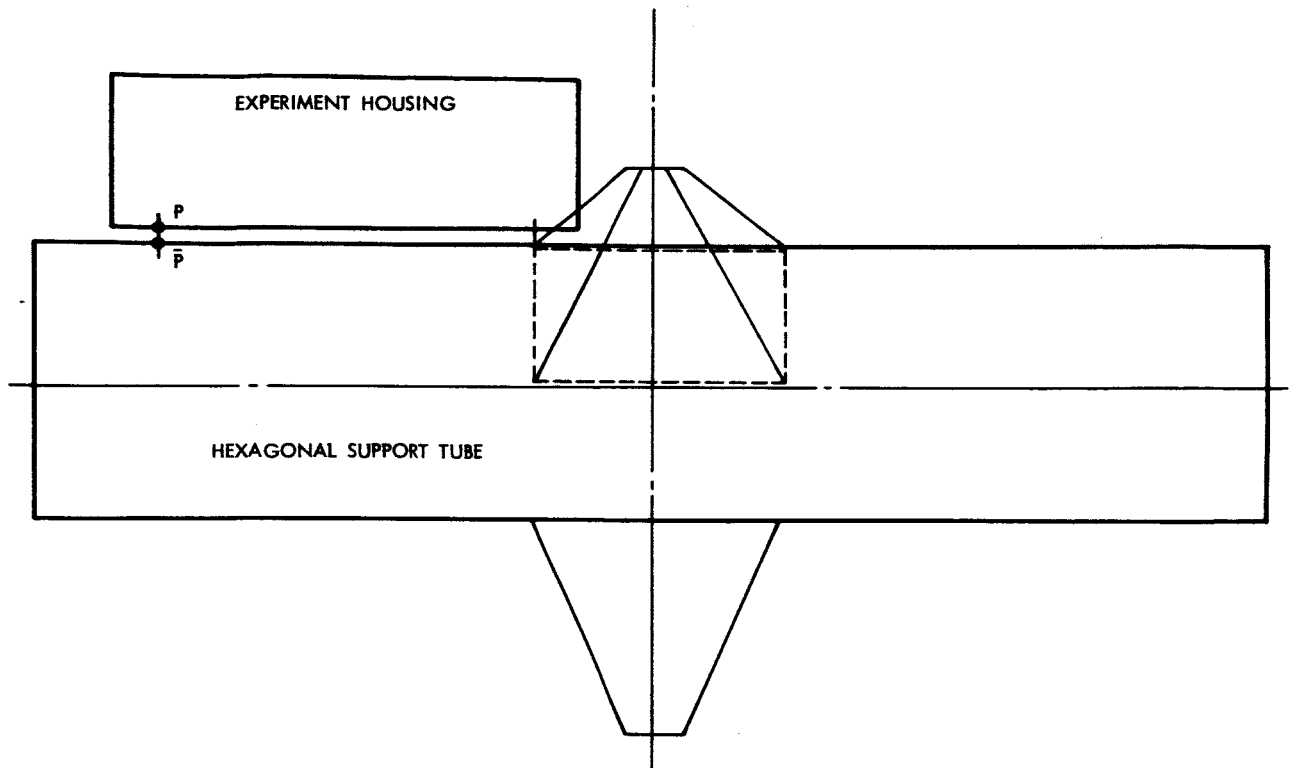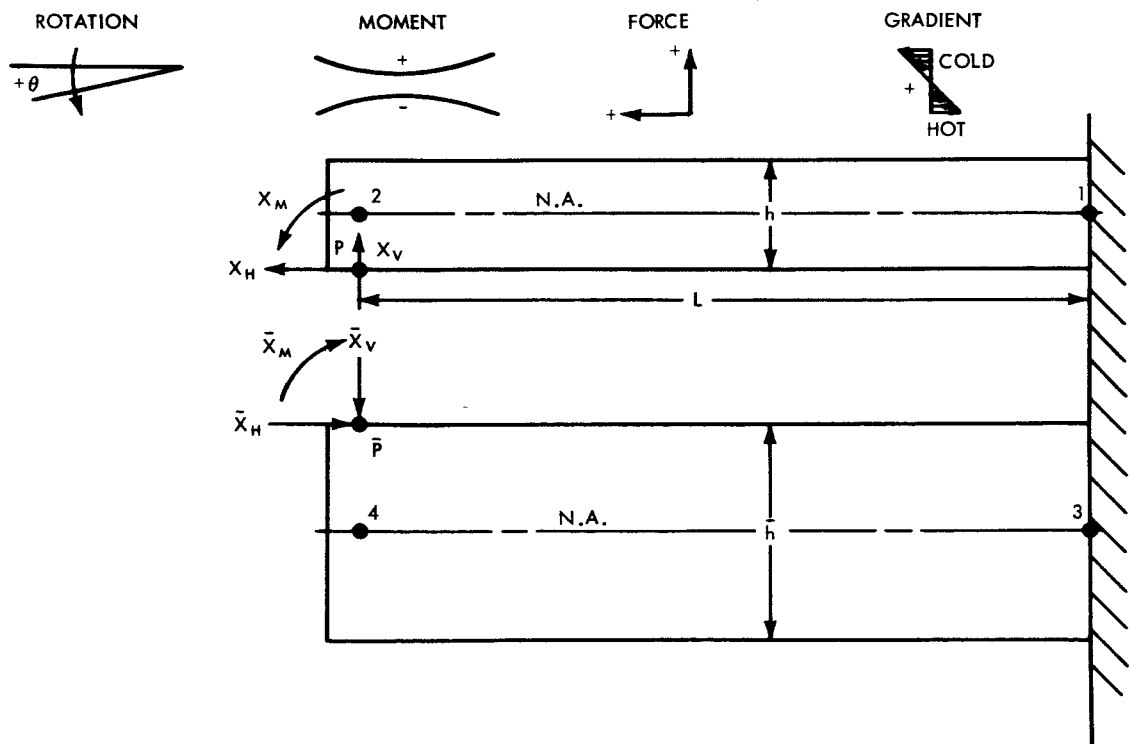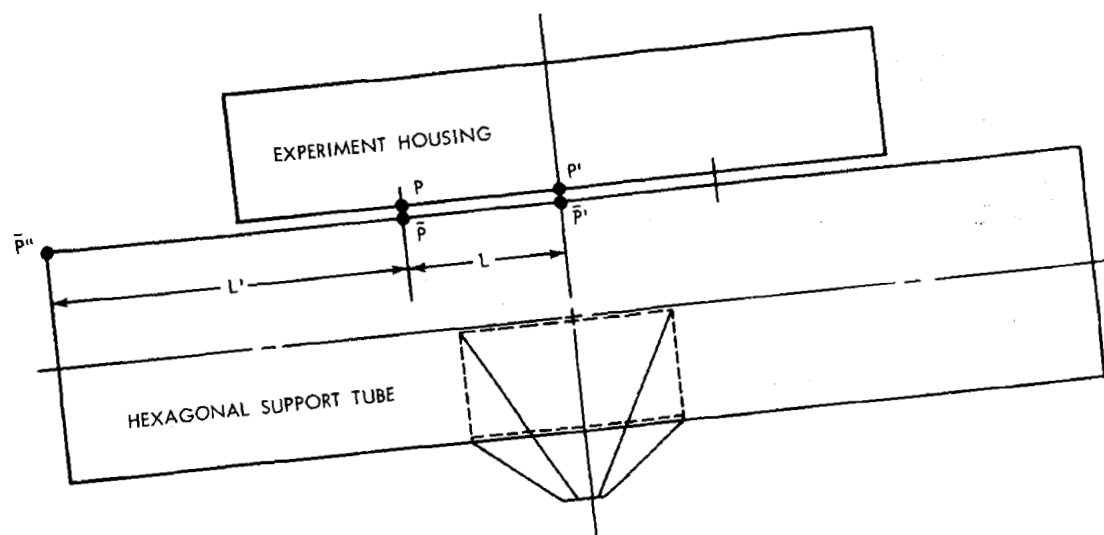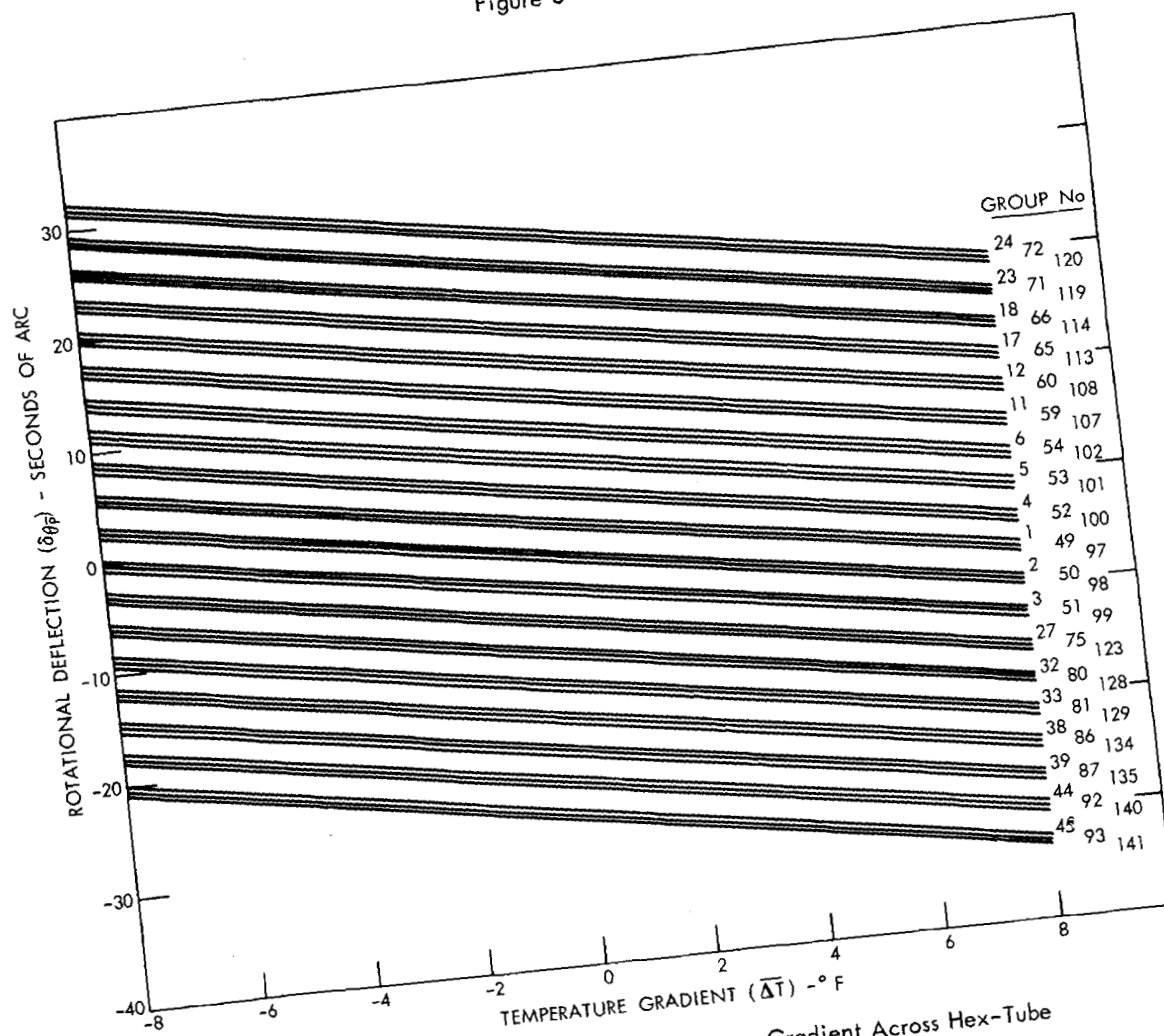
Figure 1

Figure 2

Figure 3

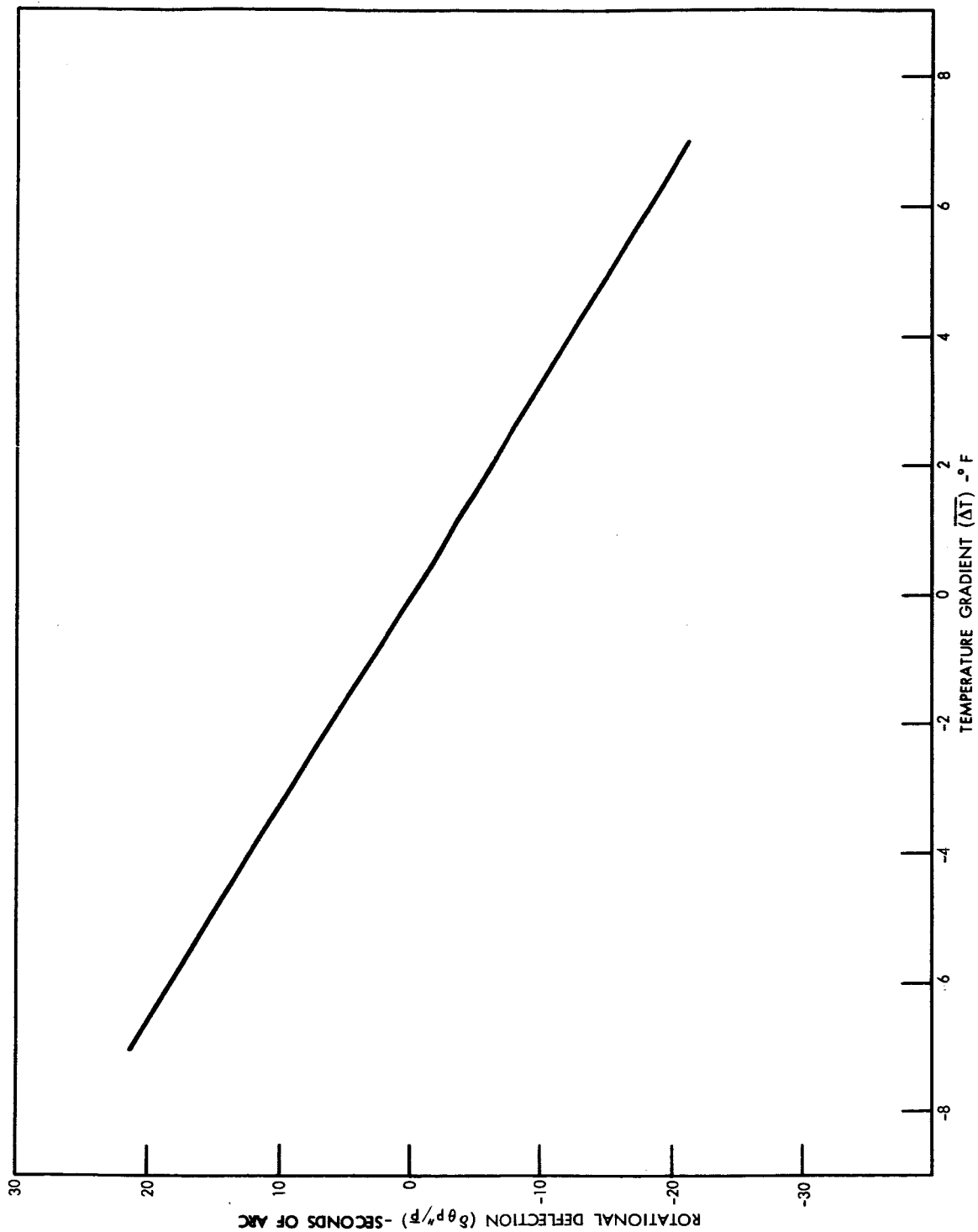Figure 4—Variation of DEFHEX with Temperature Gradient Across Hex-Tube for all Groups of Run No. 1.

Figure 5—Variation of DEFREL with Temperature Gradient Across Hex-Tube for all Groups of Run No. 1.
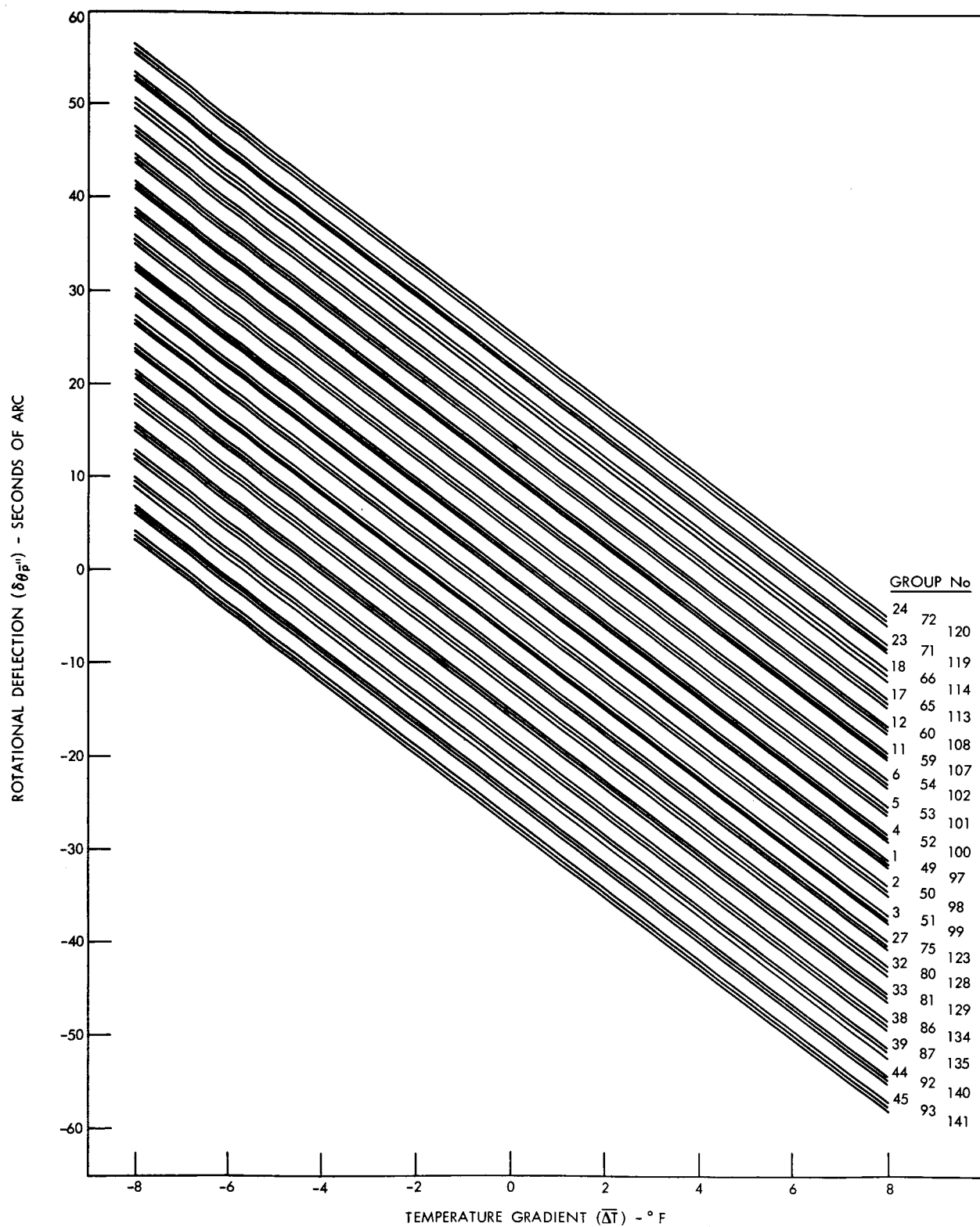
29

Figure 6—Variation of DEFEND with Temperature Gradient Across Hex-Tube for all Groups of Run No. 1.
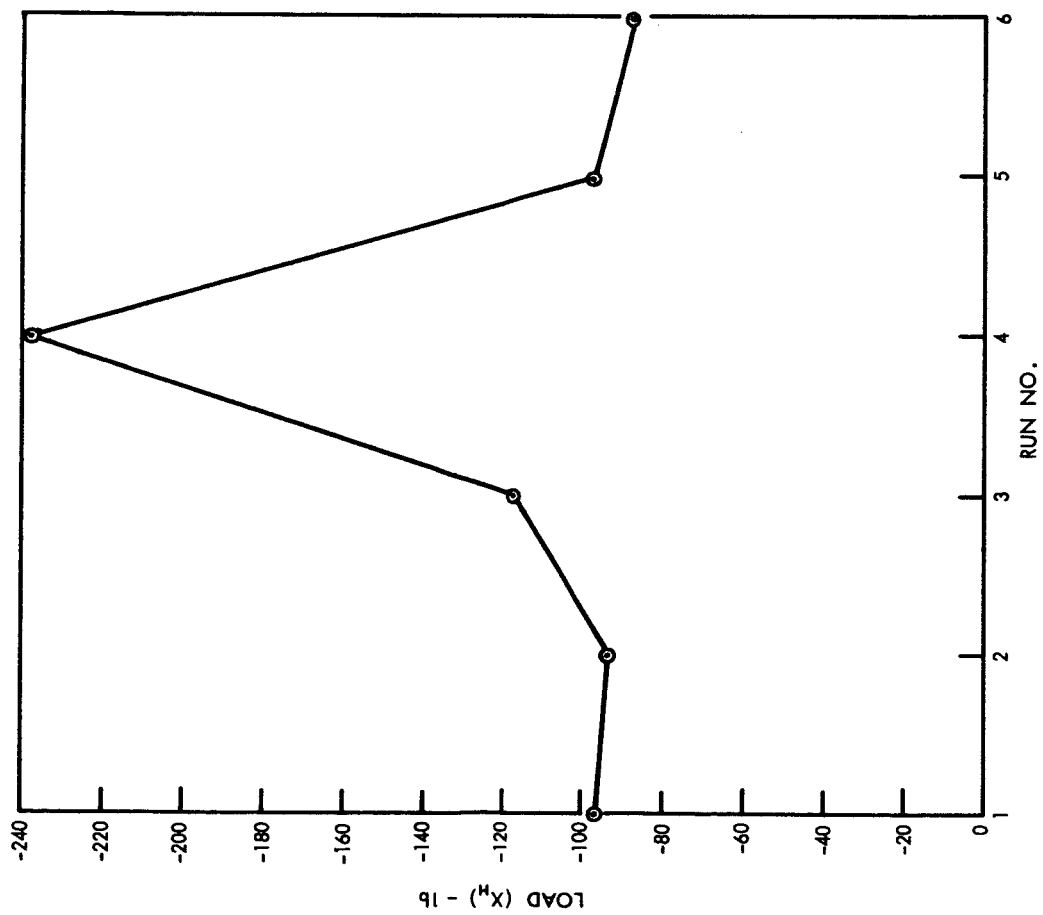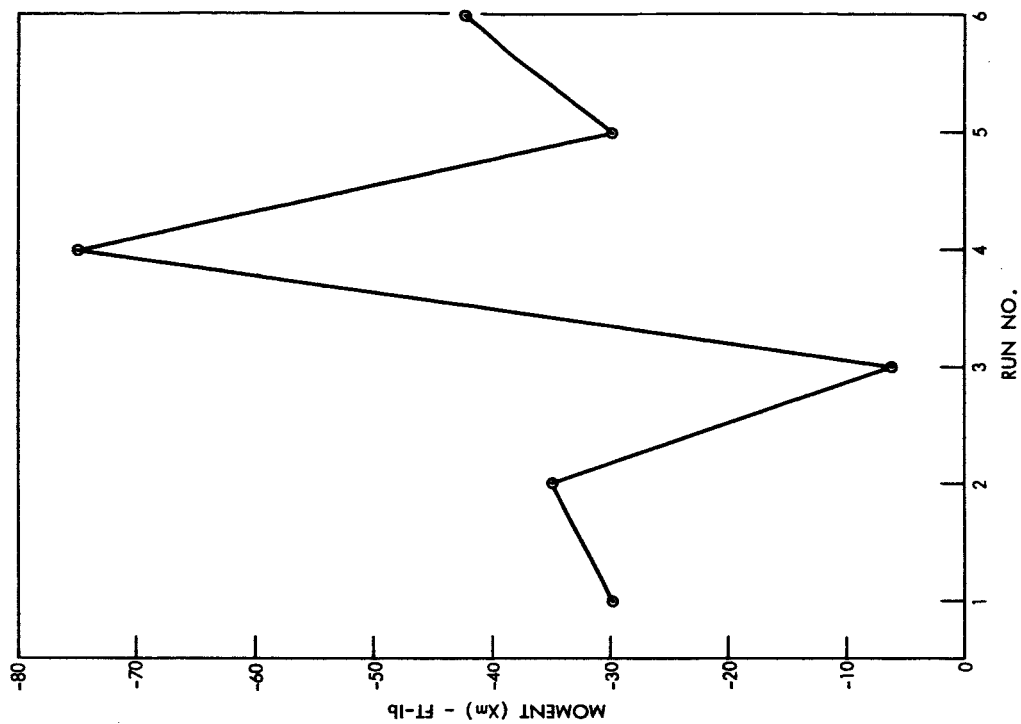
Figure 7—Longitudinal Interaction Force for Each Run.

Figure 8—Interaction Moment for Each Run.

31